

TECHNICAL PAPER

Overlapping Lattice Modeling for concrete fracture simulations using sequentially linear analysis

Beyazit B. Aydin | Kagan Tuncay | Baris Binici 

Department of Civil Engineering, Middle East Technical University, Ankara, Turkey

Correspondence

Baris Binici, Department of Civil Engineering, Middle East Technical University, Ankara, Turkey.

Email: binici@metu.edu.tr

Funding information

Scientific and Technological Research Council of Turkey (TÜBİTAK), Grant/Award number: 215 M870

Modeling concrete fracture is important in order to uncover accurately the sources of distress which lead to the damage or failure of structures. Many different numerical approaches have been used in the past employing either a smeared or a discrete cracking approach. Those models have difficulty in capturing the local nature of cracking, as well as the direction of crack propagation. Lattice modeling and peridynamics (PD) are some of the more recent nonlocal fracture simulation tools which possess advantages, such as ease of modeling and accuracy of crack propagation simulations with few key parameters. In this work, we employ an overlapping lattice approach, where the continuum is discretized using truss elements extending over a predefined horizon similar to the concept used in PD with the sequentially linear analysis technique. Simulation results for several reinforced concrete (RC) and un-RC tests demonstrate the ability to estimate crack propagation directions and widths accurately, with the proposed modeling approach also offering a rather simple and intuitive approach.

KEY WORDS

concrete fracture, lattice modeling, tension softening

1 | INTRODUCTION

The analytical simulation of concrete is very important for the structural engineering community as the key reasons of the aging infrastructure in many countries, creating billions of dollars' worth of repair and replacement costs,¹ are associated with concrete cracking. Computational models for structural concrete subjected to extreme and environmental loads must give results with reasonable accuracy for the performance evaluation, repair, strengthening of existing structures, or the design of modern ones. In this way, it is possible to attain economical engineering solutions.

Starting from the 1960s, concrete finite element simulations were conducted in the two mainstream directions. The first approach was based on the adjustment of adjusting the material stiffness matrix (i.e., smeared crack concept) introduced by Rashid.² Later, Hillerborg³ and Bažant and Oh⁴ led the development of stress-displacement models, which were used to regularize mesh dependency through a characteristic length scale and the fracture energy.^{5–7} There are

essentially two methods for the smeared crack models, that is, rotational^{5,8} and fixed crack models^{9,10} in order to estimate crack initiation and propagation directions. The main drawback of the continuum-based finite element modeling is the inability of representing the actual separation due to cracking and having to operate with average strains across a gauge length rather than with actual crack openings. The second approach for concrete fracture simulations is the use of discrete crack models by placing springs, interfaces, or contact elements between the finite elements to mimic the separation and crack opening.^{11–14} Despite the apparent advantages of modeling, the cracks via discrete elements explicitly, the issues on identifying crack locations as *a priori*, remeshing, pre and postprocessing, and the necessity of defining different constitutive models for the cracks and continuum parts are the key disadvantages of discrete crack models.

Lattice-based simulation techniques have started to become popular for concrete fracture simulations in the last two decades. The lattice approach by employing truss or

beam elements to model the continuum and simulate fracture has been used by many researchers (see, e.g., Schlangen and Van Mier,¹⁵ Tuniki,¹⁶ Van Mier).¹⁷ These works attempted to simulate the quasi-brittle response by removing elements from the system after reaching a critical strain. The lattice model was also used at the mesoscale level by others (e.g., Cusatis et al,¹⁸ Van Mier)¹⁷ explicitly modeling aggregates, cement paste, and interfacial transition zones separately with different material constants. More practical and design oriented models such as the strut and tie model of Schlaich et al¹⁹ can also be thought as a truss network approach applied at a larger scale. Hence, a lattice network, initially proposed in the 1940s by Hrennikoff,²⁰ can be considered as a multi-scale approach to concrete simulation.¹⁷

The bond-based peridynamics (PD) of Silling,²¹ which followed a particle interaction approach, can be seen in the same line of development. In the bond-based PD, each point interacts with neighboring points with a pairwise force function and the damage is incorporated by allowing bonds to break when the elongation exceeds a threshold value. For materials that exhibit tension softening, the bond force can be a nonlinear function of elongation. The bond behavior in PD is in fact similar to the constitutive model of a truss member. Recently, a number of models have been developed and verified for nonlinear problems by using PD.^{22–24} These results further support the possibility of modeling a continuum with a bond (or lattice) network, while incorporating the damage associated with cracking inherently.²⁵

This study provides a new approach named as the overlapping lattice model to simulate autonomous fracture initiation and propagation. It follows the truss network analogy to model the concrete and borrows the idea of using different horizons in connecting nodes from PD. We work at the mesoscale level (i.e., few millimeters of mesh resolution); however, we treat the concrete continuum as a single-phase medium so as to preserve practicality. Differently from the approaches presented in the literature, a new calibration approach is presented for the tension softening response of members while retaining grid size objectivity. The sequentially linear analysis (SLA) technique is employed for all simulations.

In short, the proposed approach has the following new features: (a) the horizon concept from PD is used along with lattice network approach, (b) the constitutive models of the mesoscale truss elements are back calculated by using the average measurements from the direct tension tests, (c) the continuous media are modeled using overlapping lattice elements with uniform material properties, thus retaining simplicity for parameter calibrations. After calibrations with material tests, a number of validation studies are conducted by using the results of a notched beam bending test, a scaled dam test, a tension stiffening test for a reinforced concrete (RC) member and an RC beam.

2 | OVERLAPPING LATTICE APPROACH WITH SLA

2.1 | Modeling

Nonlocal theories consider the effects of long-range interactions in solid materials. Their application to problems of solid and fracture mechanics has been studied in depth by Kröner,²⁶ Eringen,²⁷ and Kunin.²⁸ Constitutive relations are typically written in an integral form that can be expanded in a series of spatial derivatives of strain accounting for gradients and higher gradients of strain. The term “nonlocal” indicates that stress at a point depends on strain as well as gradients of strain at the same point. In the proposed overlapping lattice model, each node interacts with points within a predetermined distance called the horizon (δ) to account for the nonlocal effects, that is, the effect on a point from the immediate surrounding points. For the two-dimensional problems defined with uniformly distributed particles separated by d in the x , y directions, a particle located away from boundaries is connected to 8 and 28 nodes for horizon values of $1.6d$ and $3.01d$, respectively. The connected points are those within a circle for a selected horizon distance as shown in Figure 1a,b. In this study, we use a classical structural analysis approach to treat the interaction forces between nodes by employing classical two-node truss elements similar to Macek and Silling²⁹ as opposed to the explicit integration commonly used in particle-based dynamic simulations. Each point is initially connected to all points within its horizon via truss elements that can only transfer axial load and have the same elasticity modulus for tension and compression. The force in truss elements is assumed to behave linearly until the critical strain ε_{cr} is reached. As concrete exhibits tension softening, beyond this critical strain, the element can transfer further tension by softening as shown in Figure 1c. The modulus of elasticity times the cross-sectional area of truss elements ($E_t A_t$) in the lattice model is obtained by using a simple energy principle. First, we introduce a deformation field (e.g., a constant strain field in the x direction, $\varepsilon_x = \text{constant}$, $\varepsilon_y = 0$) and calculate the total elastic energy (E_{or}) stored in the original problem using the actual modulus of elasticity of concrete. Then, the same deformation field is applied to the lattice model and the total elastic energy (E_{ol}) calculated by taking $E_t A_t = 1$. As the stored energy is proportional to $E_t A_t$ in the lattice model, $E_t A_t$ is found by dividing E_{or} by E_{ol} . The nonlinear tension softening part is assumed to be in the form of a stepwise linear softening function as shown in Figure 1c. Concrete in compression is assumed to be elastic as concrete crushing was not the cause of failure in any of the problems investigated.

The overlapping lattice model employs simple rules for the force–deformation response of the truss elements; however, the end result is dictated by the complicated connectivity and damage sequence of the truss elements. Being a

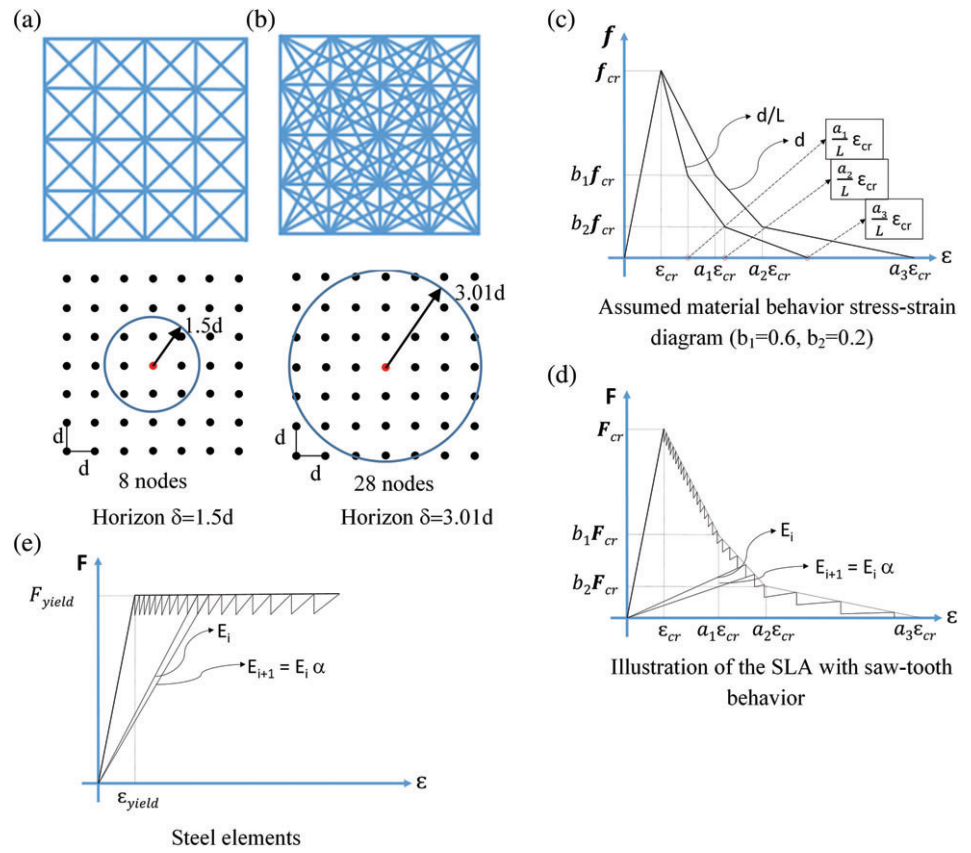


FIGURE 1 Horizon scheme, material behavior, and saw-tooth behavior

mesoscale approach (i.e., an element size of the order of a few millimeters), the force displacement responses of the concrete ingredients are needed to relate the meso and macroscale response. It is possible to model the mesoscale response of cement paste, aggregates, and interfacial transition zone by using the overlapping lattice model. Despite its potential of capturing the crack propagation better within the cement paste, such an approach requires many parameters to be able to describe the geometry and mesoscale ingredients. Instead of attempting to link the mesoscale response to the concrete medium, we prefer an engineering approach, where the truss elements are assumed to have similar force-deformation response curves representing a homogenized continuum. In this way, a more practical modeling approach capable of simulating concrete fracture (as shown in the later sections) with a reasonable engineering accuracy is achieved.

2.2 | Sequential linear analysis (SLA)

In order to solve the nonlinear response of the system modeled with an overlapping lattice approach, methods such as Newton–Raphson, arc length methods etc. are commonly employed. Such algorithms are prone to convergence problems due to severe softening and snapback responses that can be observed in the simulation of quasi-brittle materials. In order to overcome these limitations, the response of the overlapping lattice model in this study was solved by using the SLA as proposed by Rots.³⁰ SLA is a simple and robust

solution method for severely nonlinear problems as there are no convergence problems due to the softening. Furthermore, SLA is easy to program as it only requires elastic analysis with no iterations and is capable of obtaining the response even with snapback. The analysis results are usually jagged due to the sequential elastic nature of the analysis and the solution is accepted as the envelope of the response curve. In SLA, the analysis sequence was controlled by the damage imposed on the most critically stressed element as opposed to direct force or displacement control. The summary of the analysis procedure may be outlined as follows:

- i. Conduct a linear elastic analysis of the overlapping lattice model under the given reference loads and find the truss element with the highest demand capacity ratio (force in the bar/tensile strength of the bar),
- ii. Reduce the stiffness of the most critical element following the saw tooth curve given in Figure 1d,
- iii. Perform the analysis with the modified stiffness for the damaged element,
- iv. Conduct steps i-iii repeatedly such that damage is induced incrementally by reducing the effective modulus of elasticity of all critically stressed elements.

A computer program was prepared to automatically create the overlapping lattice model with a predetermined element size and horizon and to conduct SLA steps with a preconditioned conjugate gradient iterative solver.

2.3 | Parameters

The input material properties needed for the overlapping lattice simulations are E_t , the tensile strength (f_{cr}), and the fracture energy (G_f) usually obtained from material tests. In addition, the multilinear softening function parameters (shown in Figure 1c) of the truss elements are also required for the overlapping lattice simulations. Our preliminary simulations revealed that the softening function of truss elements, when selected from the available softening models in the literature, cannot provide accurate tensile response predictions mainly due to the local nature of the overlapping lattice model. It is well known that all available softening models were derived from average displacement measurements from tension tests and cannot reflect the mesoscale response of concrete in tension. Furthermore, the softening parameters cannot be directly taken from a typical tension test due to the absence of reliable test data with densely located local displacement measurements similar to the overlapping lattice grid. Therefore, tensile stress-average displacement (within a specific gauge length) curves were employed to calibrate the multilinear softening function parameters. For direct tension tests performed by Gopalaratnam and Shah (GS)³¹ and Cornelissen et al (COR)³² (COR), tensile-average displacement curves were taken from experiment results whereas for other tests, Equation (1) was used as the relationship for the pseudo-experimental results. For different grid sizes, the length scale was then used to adjust the input stress-strain function similar to the approach used in the mesh regularization in finite element simulations.⁴ Afterwards, structural member simulations were performed by using the input material properties and calibrated softening function parameters.

3 | UNIAXIAL TENSION TEST CALIBRATIONS

The first set of calibrations were performed by using the tension test results of GS³¹, and COR.³² E_t , f_{cr} , and G_f values were taken as 29.1 GPa, 3.41 MPa, 0.054 kN/m for GS³¹ and 21.0 GPa, 3.47 MPa, 0.1 kN/m for COR³² as reported in their tests. The tension test specimens for these two problems have notch heights of 3 mm (GS) and 5 mm (COR) and widths of 13 mm (GS) and 5 mm (COR). The measurement gauge lengths of the experiments were reported as 83 mm (GS) and 35 mm (COR). The experiment test setup/specimens for GS³¹ and COR³² are provided in Figure 2. The test specimens of GS and COR were first modeled with a grid spacing (d) of 1 and 2.5 mm, respectively. Afterwards, the optimum parameters for a_1 , a_2 , a_3 , b_1 , and b_2 that minimize the difference between the reported and computed fracture energies were determined for an error tolerance of 10%.

In order to minimize the mesh size dependency, fracture energy regularization was employed. For an overlapping lattice model with a grid spacing of d , the softening function parameters of a truss element with a length of L (i.e., different than the grid size), were multiplied with d/L (Figure 1c). In this way, the area under the stress-displacement response for each truss member was similar. This scaling was also applied in the case of using a grid size different than d to ensure the incorporation of a size effect similar to previous studies.^{6,33–35}

Calibrated parameters a_1 , a_2 , a_3 for different specimens and horizons are presented in Table 1 for a grid spacing (d) of 1 mm. Interestingly, the values of b_1 and b_2 were found

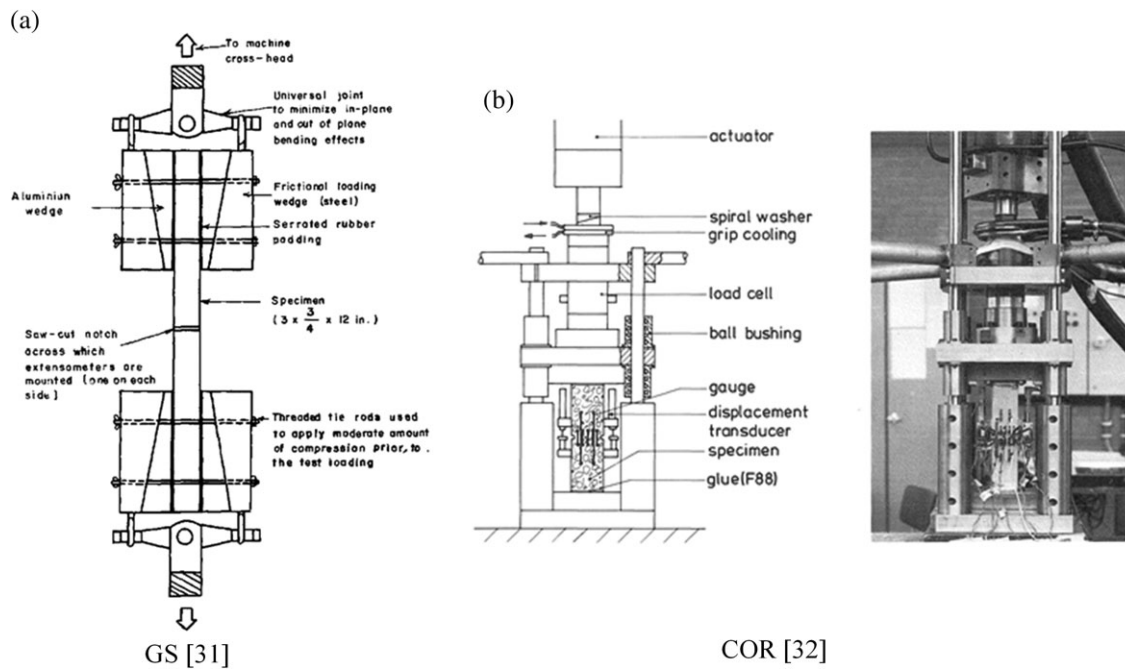


FIGURE 2 The experiment test setup/specimens for Gopalaratnam and Shah³¹ (GS) and Cornelissen et al³² (COR)

as 0.6 and 0.2, respectively, regardless of the fracture energy, horizon, or mesh size. The comparisons of the experimental and analysis results for the stress–deformation responses are presented in Figure 3 and the damage patterns at the end of simulations are shown in Figure 4. In the figure, color contours denote the strain value of elements ranging from the cracking strain to 0.02. The amplification factor for the deformation field presented for the notch region was taken as 20 for illustration purposes. Furthermore, for coarse grids whose length exceeds the notch height, the elements that fall in the notch region were weakened by multiplying the ϵ_{cr} value with an appropriate small number to account for the notch geometry. Close agreement between the test and simulation results was observed even with significantly large grid spacings. It is interesting to note that the mesh regularization by scaling the softening function appeared to provide objective results while slight differences in the response estimations stemmed from the inability of placing the notch accurately when the mesh sizes were larger than the notch depth.

The analysis results upon increasing the horizon for the two cases are presented in Figure 5 along with the damage patterns in Figure 6. It should be noted that the use of a longer horizon required the change only of a_1 among all parameters as shown in Table 1 in order to match the test results with a reasonable engineering accuracy. The results for the $3.01d$ horizon results had different crack patterns compared to cases with $1.5d$ as the cracks tended to extend beyond the notch region. This was due to increasing nonlocal effects, which tended to

diffuse the crack beyond the notch region. The key reason for this situation was the presence of long diagonal elements connected from the notch region to the region outside the notch. This is surmised to be the reason for spreading of the cracking and misrepresentation of the nonlocal damage interactions. In order to objectively observe the effect of horizon on the tension test results, a numerical experiment was conducted on a specimen with a relatively large notch as shown in Figures 7 and 8. In this way, it was ensured to have a sufficiently dense mesh within the notch region with a reasonable element size. E_t , f_{cr} , G_f , and the gauge length values were taken as 27.0 GPa, 3.1 MPa, 0.07 kN/m, and 48 mm, respectively. The stress-displacement model of COR³² given in Equation (1) was employed as the “correct” test result for the softening part and the calibration of the input parameters were conducted based on those results

$$\frac{f(u)}{f_{cr}} = \left(1 + \left(c_1 \frac{u}{u_{ult}} \right)^3 \right) \exp\left(-c_2 \frac{u}{u_{ult}} \right) - \frac{u}{u_{ult}} (1 + c_1^3) \exp(-c_2), \quad 0 < u_n < u_{n,ult}. \quad (1)$$

In the above expression, f_{cr} is the uniaxial tensile strength, and c_1 and c_2 values are the constants taken as 3 and 6.93, respectively. u_{ult} is the ultimate displacement, (taken as $5.136 * G_f / f_{cr}$) and u is the average crack displacement within the gauge length. The measurement gauge length for the numerical experiment was taken as 48 mm while comparing the results with those from Equation (1). The stress–deformation results and the damage patterns are presented

TABLE 1 Parameters for tests for $d = 1$ mm (unit of all G_f value is N/m)

GS ³¹	COR ³²	Numerical	Petersson ³⁶ $G_f = 124$	Petersson ³⁶ $G_f = 150$	Dam $G_f = 60$	Dam $G_f = 100$	Dam $G_f = 150$	Tension stiffening $G_f = 60$
$\delta = 1.5d$								
a_1	6.6	9	6.4	7.5	7.5	15	12.5	10
a_2	75	100	120	200	250	30	60	125
a_3	450	700	600	1,200	1,400	300	500	650
$\delta = 3.01d$								
a_1	12	12.5	12.4	15.5	15.5	20	17.5	15.5
a_2	75	100	120	200	250	30	60	125
a_3	450	700	600	1,200	1,400	300	500	650
								1,000

GS = Gopalaratnam and Shah³¹; COR = Cornelissen et al.³²

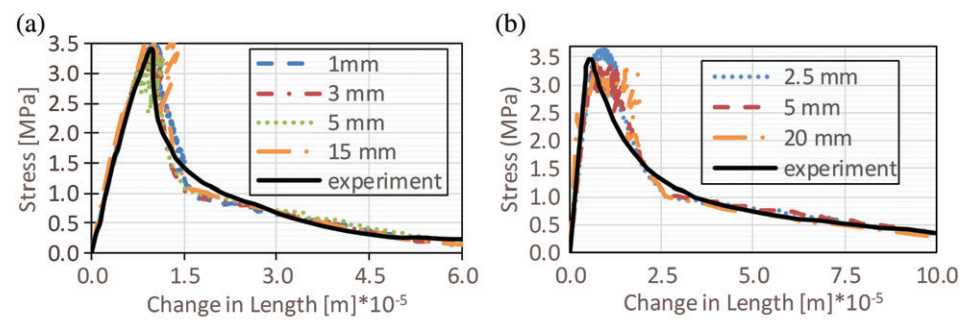


FIGURE 3 Force–deformation curves for horizon = $1.5d$ for Gopalaratnam and Shah³¹ and Cornelissen et al³²

GS

COR

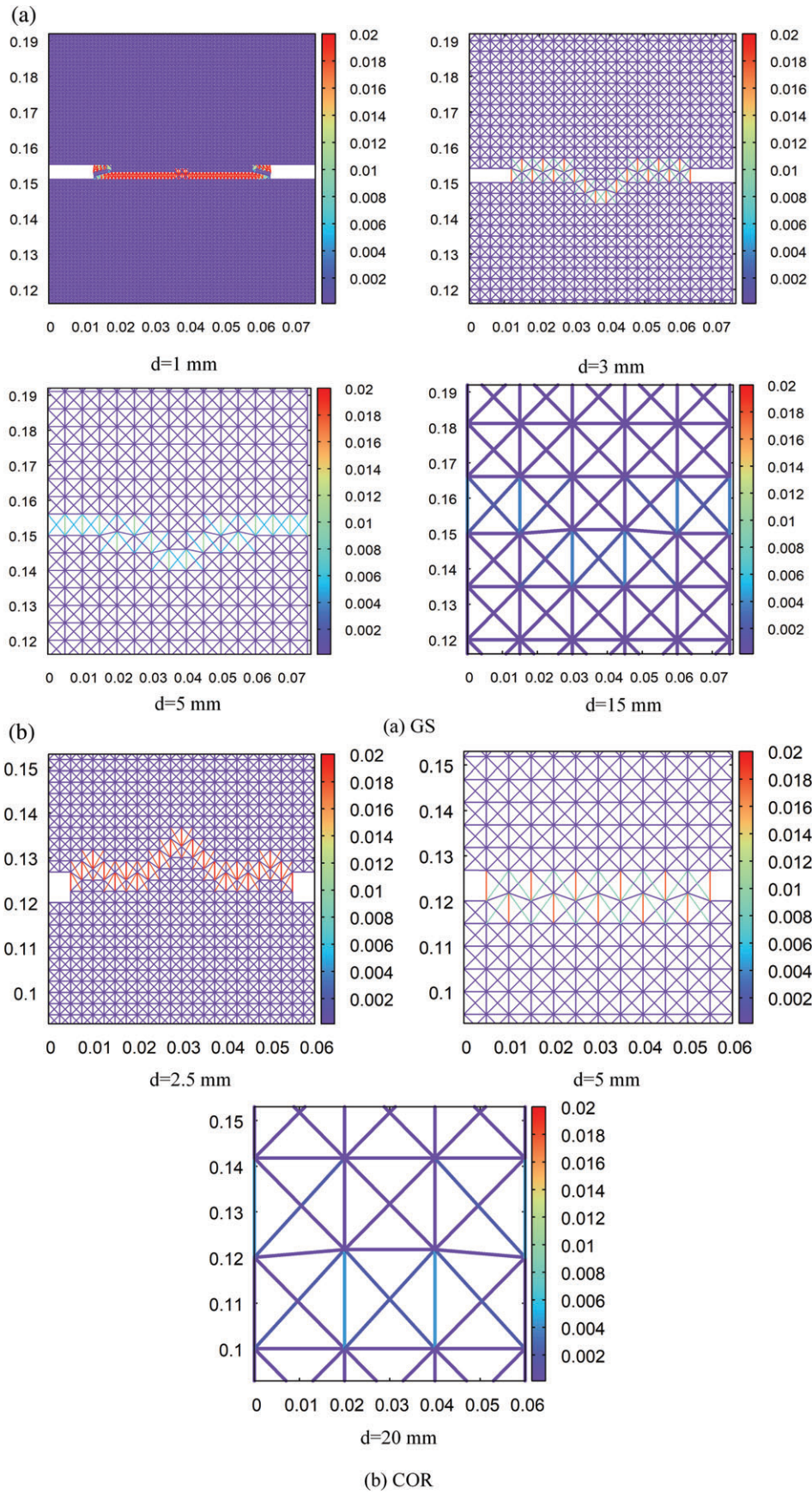


FIGURE 4 Damage patterns with different initial spacings with horizon = $1.5d$ for Gopalaratnam and Shah³¹ and Cornelissen et al³²

in Figures 7 and 8, respectively. These numerical experiments reveal three important conclusions: (a) the increase of the horizon seems to provide a better match

for the softening part resulting in a better representation of the coalescence of cracks, (b) the mesh regularization upon scaling the input softening function for different

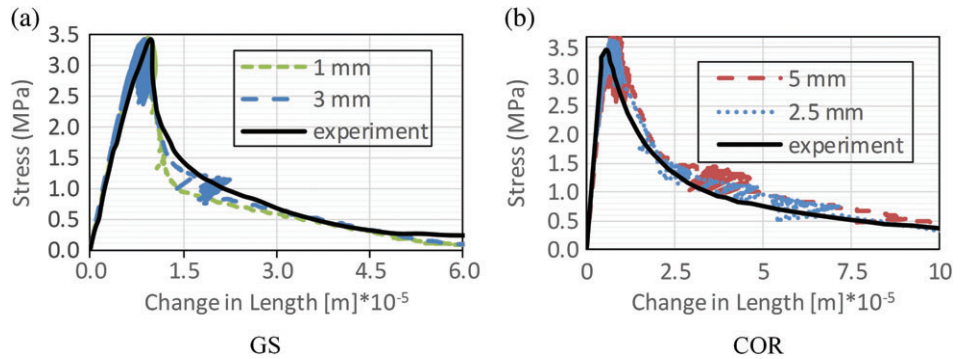


FIGURE 5 Force–deformation curves for horizon = $3.01d$ for Gopalaratnam and Shah³¹ and Cornelissen et al³²

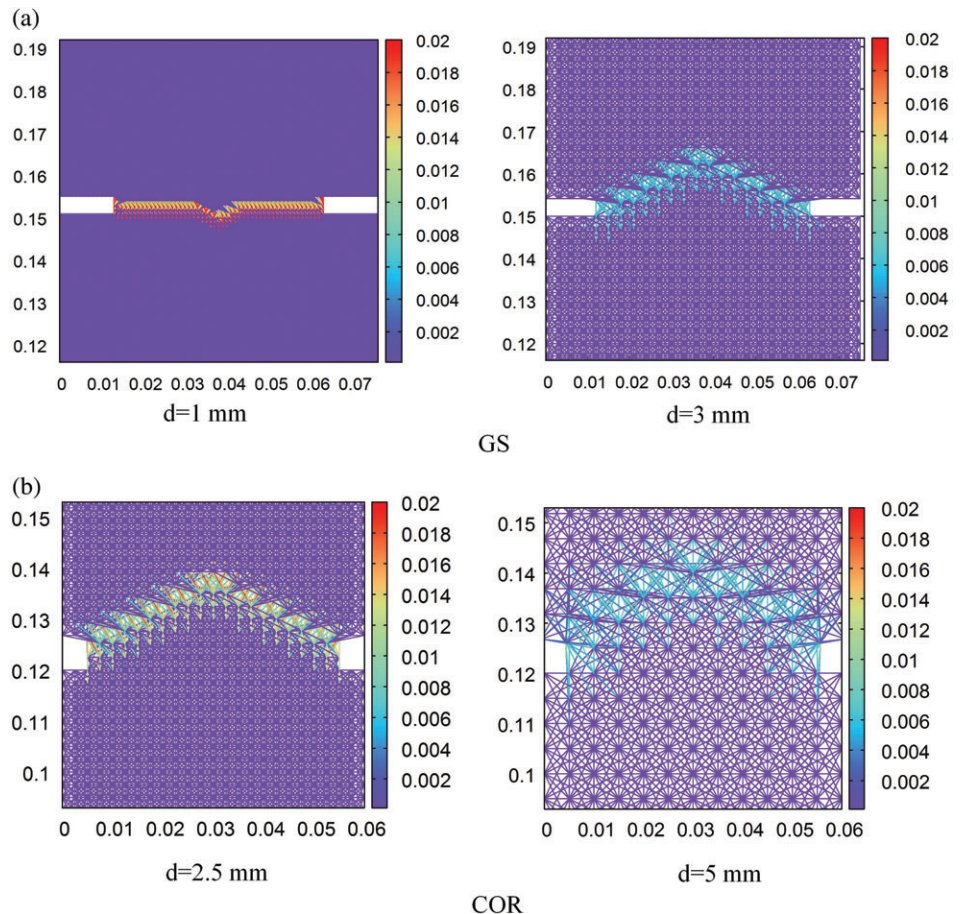


FIGURE 6 Damage patterns with different initial spacings with horizon = $3.01d$ for Gopalaratnam and Shah³¹ and Cornelissen et al³²

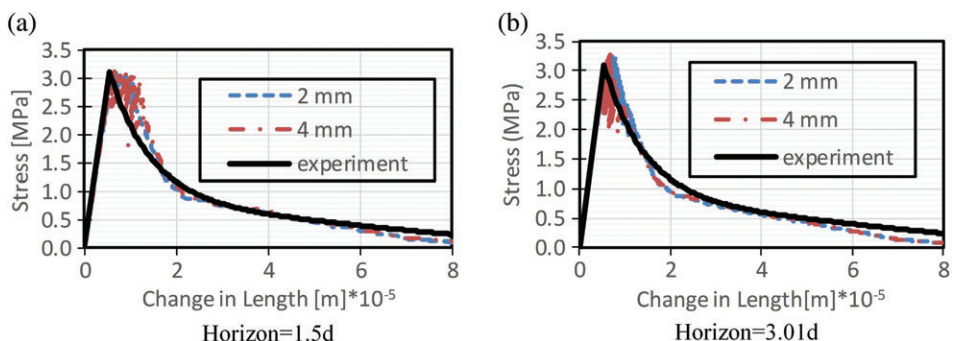


FIGURE 7 Force–deformation curves for $d = 2$ mm and $d = 4$ mm for numerical tests

mesh sizes seems to be successful, (c) use of a sufficiently small mesh within the notch region is important in order to capture the load–deformation response in

direct tension tests. These results provide confidence on the ability of estimating cracks for concrete in tension tests while accurately modeling the average stress–

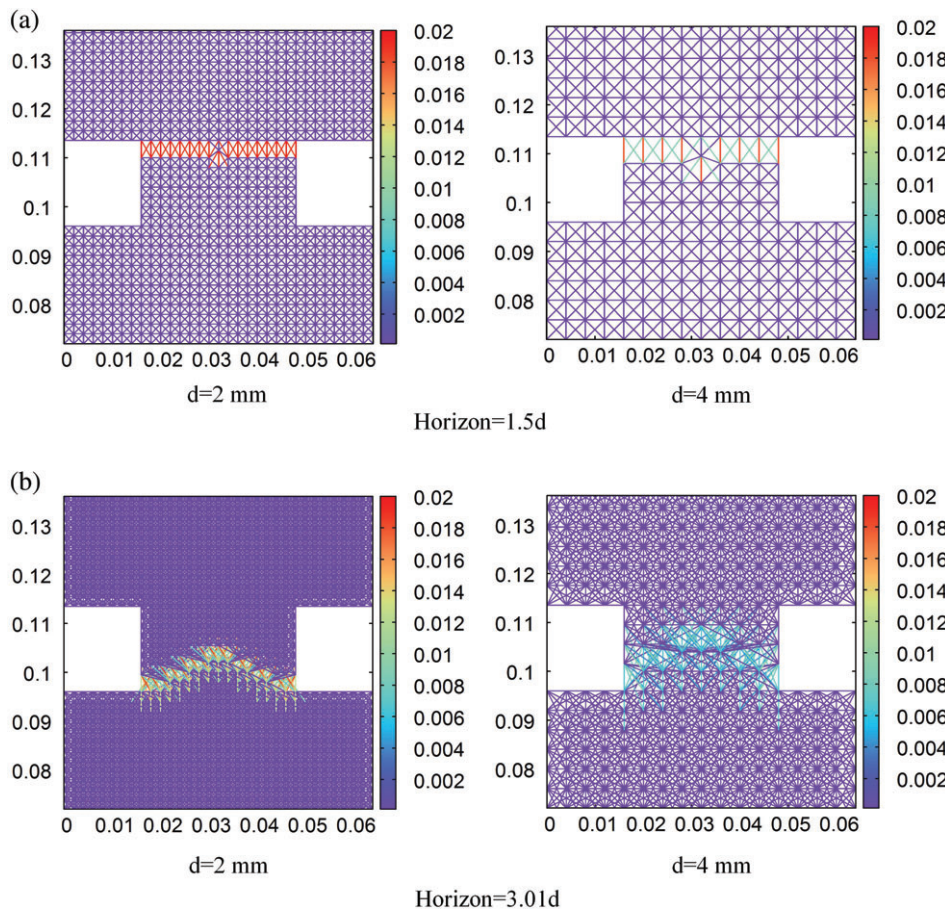


FIGURE 8 Damage patterns for $d = 2\text{ mm}$ and $d = 4\text{ mm}$ for numerical test

displacement response with the overlapping lattice approach.

4 | VALIDATION OF THE OVERLAPPING LATTICE MODEL WITH STRUCTURAL MEMBER TESTS

4.1 | Notch beam test

The three-point bending experiment (Figure 9a) performed by Petersson³⁶ was simulated in order to assess the performance of the overlapping lattice approach for a bending-induced crack propagation problem. E_r , f_{cr} , and G_f values were taken from the test results as 30.0 GPa, 3.33 MPa, and 0.124 kN/m, respectively. First, the parameters required by the lattice elements were determined such that the numerical direct tension test results of the stress-average displacement matched with the response function in Equation (1). The numerical test was conducted for a specimen having a height of 0.305 m with a notch height of 5 mm for 1.5 d horizon and 0.315 m with a notch height of 15 mm for 3.01 d horizon similar to the procedure described in the previous section and both with a gauge length of 45 mm. The calibrated model parameters are presented in Table 1. Afterwards, the overlapping lattice model was constructed for the beam test by using the parameters (modified according to the length scale) obtained from the uniaxial tension test with

a grid size of 5 mm. The load–deflection curve results and obtained crack patterns are shown in Figure 9b–d, where the two solid lines represent the experimental results and the dashed lines represent the computational predictions for two different horizons. Considering the uncertainty in the experimental data, the computational results are in reasonable agreement with the lower bound of the experimental results. In order to observe the influence of the fracture energy on the simulation results, the analyses were repeated by keeping all the parameters with a fracture energy of 0.15 kN/m (Figure 10). It can be observed that increased fracture energy resulted in an enhanced capacity and better estimation of the load–deformation response. As such, uncertainty in the fracture energy, which is usually obtained if results from a limited number of tests are available, can significantly affect computational estimations by using the overlapping lattice model.

4.2 | Scaled dam test

A 1/75 scaled model of the 120-m-high Melen Dam (Figure 11a) was tested using three different scaled ground motions by using the pseudo-dynamic testing technique by Aldemir et al.³⁷ The original setup enabled the use of only the bottom half of the dam section and the inertial and hydrodynamic load effects were simulated using a lateral hydraulic piston. The overlapping lattice model was

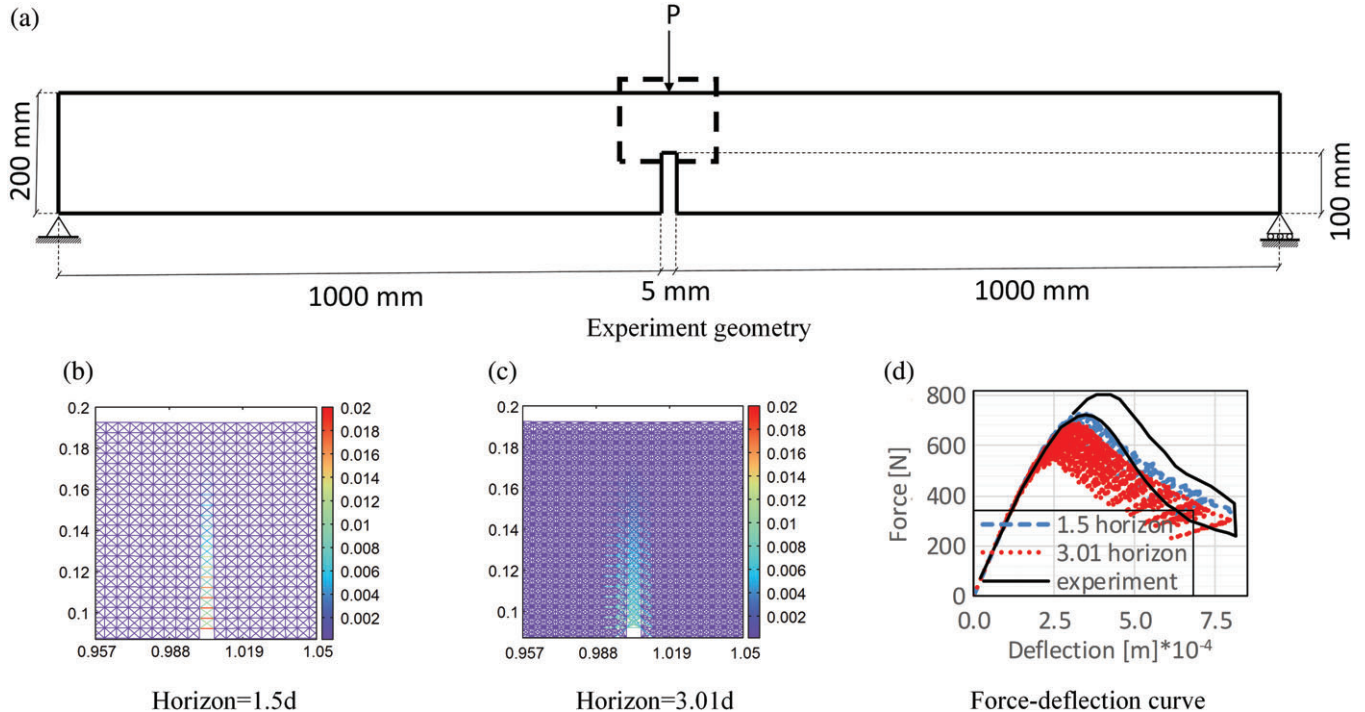


FIGURE 9 Experiment geometry, damage pattern, and force–deflection curve for $G_f = 124 \text{ N/m}$ for Petersson³⁶

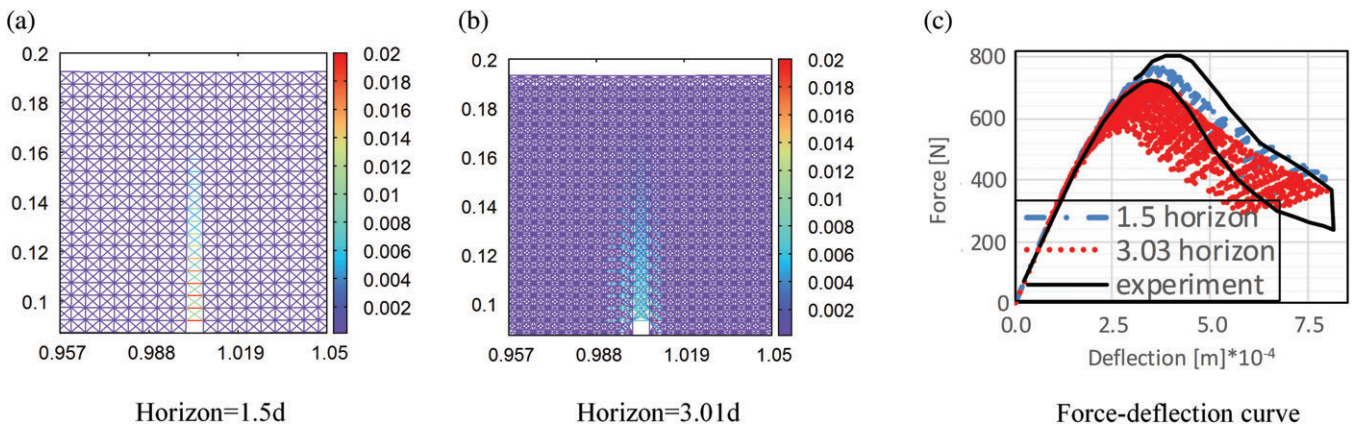


FIGURE 10 Damage pattern and force–deflection curve for $G_f = 150 \text{ N/m}$ for Petersson³⁶

constructed by using a 25-mm grid size to observe performance estimation for an un-RC structural continuum. The uniaxial material parameters for the dam simulations were obtained from the calibration of the parameters with respect to the uniaxial tension pseudo-test results (Equation (1)). This procedure is similar to the approach used for the notched beam simulations, that is, the model parameters were first estimated by using the uniaxial tension test results followed by the target simulations. As no information regarding the fracture energy value of the specimen was reported G_f values of 0.06, 0.1, and 0.15 kN/m were employed to investigate response predictions over a wide range of G_f . E_b , f_{cr} , and thickness values were taken as 10.5 GPa, 2.9 MPa, and 200 mm, respectively, as reported in the test. The elements within the top 300 mm, equipped with a specially designed threaded steel plate in the test to enable safe load transfer on

the specimen, were assumed to remain elastic. First, a 400-kN vertical load was applied on the model. Afterwards, the model was loaded from the upstream direction in a damage-controlled manner with SLA. During the SLA steps, the stresses from the 400 kN load were taken as the initial stress conditions (Figure 11a). For all G_f values and 1.5d and 3.01d horizon size, the SLA results are compared with the consecutive PD and pushover test results in Figure 11c,d. It can be observed that the initial stiffness estimation of the specimen was perfect whereas the estimation of lateral load capacity was estimated by about 20%. The deformability of the specimen was predicted in a reasonable manner with some drop of load carrying capacity around 1.5 mm. The crack patterns are shown in the same figure for a lateral tip displacement of about 3.5 mm. The crack pattern observed from the test could be taken to agree well with the base cracking shown in

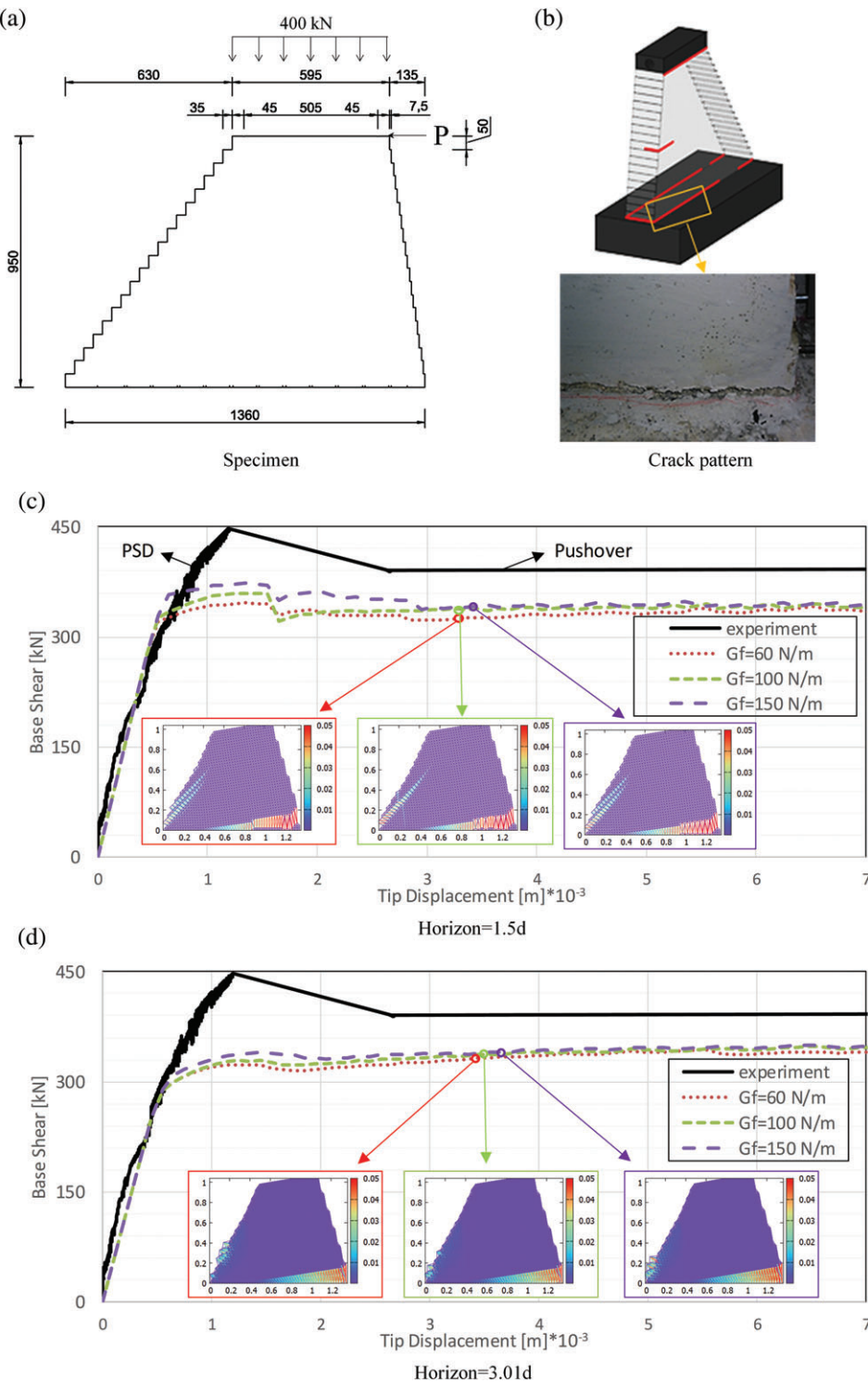


FIGURE 11 Experiment geometry and load pattern Aldemir et al.³⁷ load-tip displacement and crack pattern

Figure 11b. The computational results demonstrated the initiation of inclined split cracks in the compression zone with strains of the order of a few times the cracking strains. These cracks extending inside the dam body were not observed in the test. It is interesting to note that variation of the fracture energy or increasing the horizon value seemed to affect the response in a limited manner. This result is in contrast with the effect of fracture energy on the direct tension and bending response. The presence of axial force in addition to lateral force in the dam test is believed to reduce the effect of

fracture energy on the load-deformation behavior, which appears to follow a nearly-elastic, perfect plastic response. In short, it can be stated that the employed SLA overlapping lattice simulation was found to reproduce the overall behavior in a reasonable manner while the lateral load carrying capacity was underestimated by about 20%.

4.3 | Tension stiffening

In order to test the ability of the overlapping lattice approach in estimating the force transfer between steel

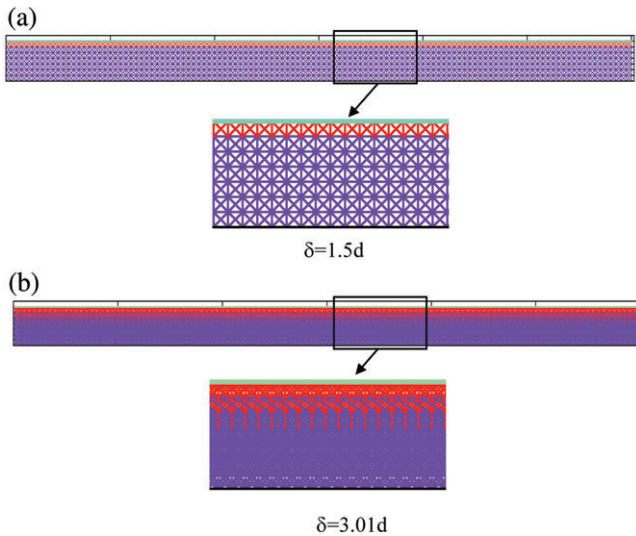


FIGURE 12 Different types of elements for both horizon sizes

reinforcement and concrete, the basic test of tension stiffening was first simulated. In this test, steel reinforcement with concrete cast around it is subjected to uniaxial tension. In this way, the ability of force transfer from steel to concrete including the axial tensile load-deformation response of concrete and associated crack spacing can be deduced. The test experiment carried out by Gijsbers and Hehemann³⁸ was used for the numerical simulations. The concrete member had a cross section of 68×68 mm with a $\phi 8$ mm rebar at the center. Half of the experiment was modeled as shown in Figure 13a by simulating with 5-mm grid size and 3.03d horizon. In order to satisfy symmetry conditions, roller supports were placed at the top boundary, and a pin support was placed at the left end of the rebar. E_b , f_{cr} , and G_f values were taken as 28.0 GPa, 2.5 MPa and 0.06 kN/m, respectively. As mentioned earlier, the softening parameters that

are given in Table 1 for this simulation were determined by finding the optimum parameters that provided the best match with the tensile stress-average displacement model of COR.³² The elasticity modulus E_s and yield stress were taken as 192.3 GPa and 400 MPa, respectively. The value of $E_r A_t$ for the truss elements representing the steel rebar was taken as half of the modulus of elasticity times the cross-sectional area of steel ($E_s A_s / 2$), where A_s was found based on 8 mm bar diameter and, due to symmetry, half of the steel area was used. In addition, there are three types of lattice elements, that is, steel reinforcement, bond, and concrete. Steel reinforcement elements were represented with a single truss element along the centroidal axis of the reinforcing bars. Bond elements were taken as all the elements connected to the steel reinforcement elements (Figure 12). For the steel-concrete interfaces, preliminary studies indicated that all connecting elements could be assumed to carry at least 70% of the tensile strength of concrete to ensure that no bond failure took place. Accordingly, an elastic perfectly plastic load-deformation response was assigned to the elements connected to steel elements such that no strength degradation (i.e., no bond failure) took place (Figure 1e). In the first stage of the experiment, tensile cracks initiated at a force level of about 13 kN whereas in the second stage of the experiment the crack widths increased and the steel rebar started taking an increasing share of the external load. Finally, the steel bar yielded when the external load reached about 20 kN. Computational results were in good agreement with the experimental results as seen in Figure 13b,c. The number of sudden drops in the force-elongation diagram which are the indicators of new crack formations also shows a fair agreement with the experimental results. These results encourage the use of the overlapping lattice approach to model RC structural

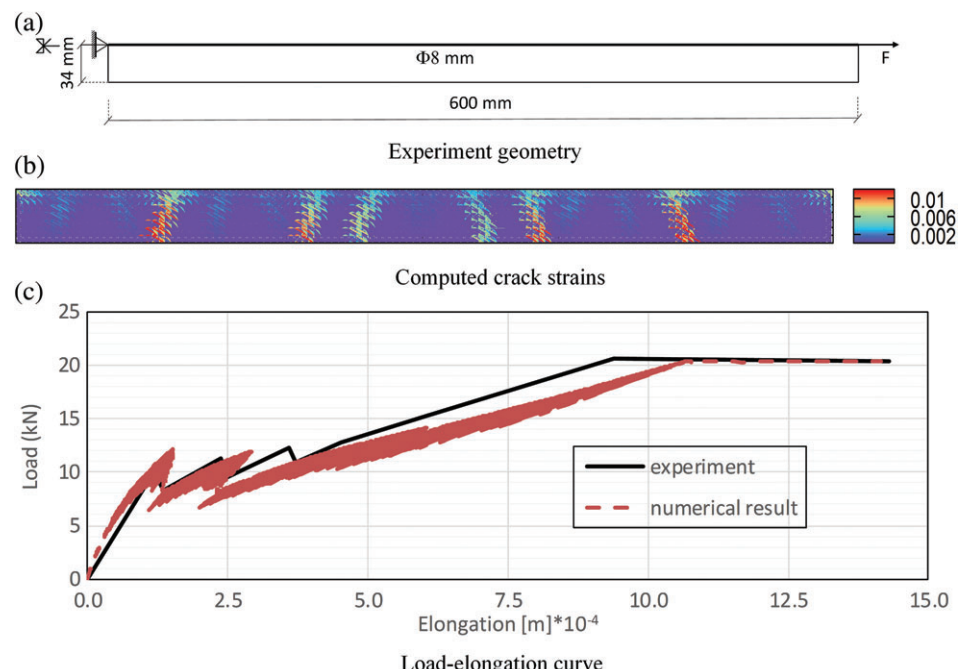


FIGURE 13 Sketch of the tension-stiffening experiment,³⁸ damage patterns, and comparison of computed and measured force-elongation diagram

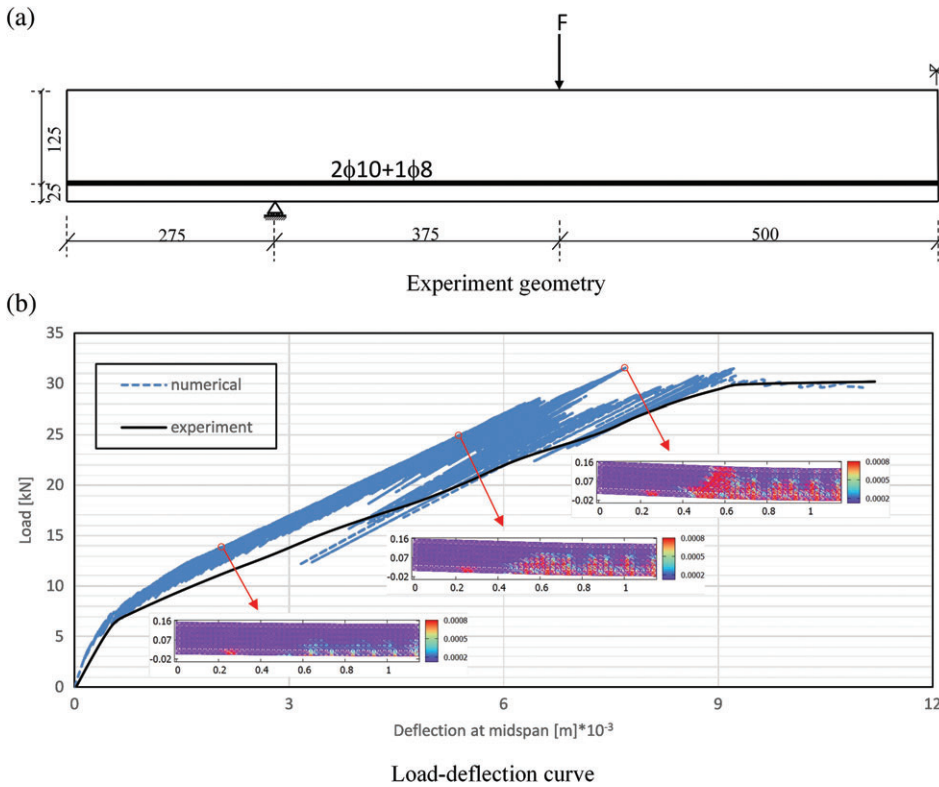


FIGURE 14 Reinforced concrete beam test³⁹ and simulation

members under loading, which is investigated with the next validation study.

4.4 | RC beam

Finally, the reinforced beam experiment tested by Walraven³⁹ was simulated by using a grid size of 25 mm with a horizon of $3.01d$. The beam thickness, E_t , f_{cr} , and G_f values were taken as 200 mm, 25.0 GPa, 2.5 MPa, and 0.06 kN/m, respectively from the reported results. The beam had a height of 150 mm and length of 2,300 mm with $2\phi 10 + 1\phi 8$ mm longitudinal rebars whose modulus of elasticity and yield stress were taken as 210.0 GPa and 440 MPa, respectively (Figure 14a). Half of the beam was simulated by placing roller supports at the right of the half beam (Figure 14a). As the fracture energy, elastic modulus and tensile strength reported by Gijsbers and Hehemann³⁸ were very close to those reported by Walraven,³⁹ the same softening parameters employed in tension stiffening were used in the simulations (Table 1). The bond elements were modeled in the same manner as mentioned in the tension stiffening simulation. The estimated load–deflection graph along with crack patterns at different loading stages is shown in Figure 14b. It can be observed that the model was capable of capturing the initial cracking load with a reasonable accuracy. Beyond that, the cracked stiffness of the specimen was slightly overestimated up until 5 mm of midspan deflection. Afterwards, the load–deflection curve obtained from the test was closely followed by the numerical results. It can be observed that the flexural cracks were spaced at

about 10 cm apart, which is the expected order of crack spacing for this beam. The ultimate capacity of the test specimen was about 30 kN, which was in perfect agreement with the test result. In short, it can be stated that overlapping lattice model was quite successful in estimating the load–deformation response of a beam failing in the flexural mode. The only shortcoming of this simulation result was that diffused crack patterns rather than discretely spaced flexural cracks were obtained.

5 | CONCLUSION

A novel approach has been proposed to simulate concrete fracture integrating the overlapping lattice model and SLA. Preliminary numerical simulations have shown that the approach has a great potential to estimate the spatial distribution and widths of cracks in both plain and RC. The horizon distance, tensile softening function, and its regularization for different mesh densities were also investigated in detail. The following key conclusions can be drawn based on these results:

- The overlapping lattice modeling is a highly nonlocal approach. This necessitates the calibration of the tensile stress–deformation response at the mesoscale in order to successfully match the macroscale response. In other words, one needs to calibrate three softening function input parameters for its members by using a

- computational direct tension test. The tensile force–deformation response is found to be sensitive to the softening function input parameters, thus requiring an objective calibration strategy.
- When the tensile force–deformation response of a tension test is calibrated, other crack propagation problems can be tackled with a reasonable level of accuracy and a lower sensitivity is necessary for the input parameters.
 - Increasing the horizon in the overlapping lattice model provides a smoother force–deformation response with a more realistic crack pattern. However, it requires a finer mesh to account for geometric irregularities.
 - The analysis of the tension stiffening and RC beam problem suggests that the force/strain curve for steel–concrete interface elements different than for concrete/concrete elements. A close match with tension stiffening and RC beam problems was obtained using elastoplastic steel–concrete interface elements with 70% of the tensile strength of concrete–concrete elements.
 - SLA provided a robust framework to analyze severely softening problems with no convergence issues, thus its use would be favorable for quasi-brittle problems.
- ## ACKNOWLEDGMENTS
- This research was supported by the Scientific and Technological Research Council of Turkey (TÜBİTAK) under grant no. 215 M870.
- ## ORCID
- Baris Binici  <http://orcid.org/0000-0002-9586-7349>
- ## REFERENCES
1. American Society of Civil Engineers. Report card for America's Infrastructure; 2013. <http://www.infrastructurereportcard.org>. Accessed August 11, 2017.
 2. Rashid YR. Analysis of prestressed concrete pressure vessels. *Nucl Eng Des.* 1968;7(4):334-344.
 3. Hillerborg A. Some practical conclusions from the application of fracture mechanics to concrete. Studies on concrete technology. Dedicated to Professor Sven G.Bergström on his 60th anniversary, Swedish Cement and Concrete Institute, Stockholm; 1979, December 14, 43–54.
 4. Bažant ZP, Oh BH. Crack band theory for fracture of concrete. *Mater Struct.* 1983;16:155-177.
 5. Rots JG. Computational Modelling of Concrete Fracture [dissertation], Delft University of Technology, Delft; 1988.
 6. Diana TNO. *Diana User's Manual*. Diana: the Netherlands; 2008.
 7. Palermo D, Vecchio FJ. Compression field modeling of reinforced concrete subjected to reversed loading: formulation. *ACI Struct J.* 2003;100(5):616-625.
 8. Vecchio FJ, Collins MP. The modified compression-field theory for reinforced concrete elements subjected to shear. *J Am Concr Inst.* 1986;83(2):219-231.
 9. Willam K, Pramono E, Sture S. Fundamental issues of smeared crack models. In: Shah SP, Swartz SE, eds. *Proceeding of SEM-RILEM International Conference on Fracture of Concrete and Rock*. Bethel, CT: SEM; 1987:192-207.
 10. Wang TJ, Hsu TTC. Nonlinear finite element analysis of concrete structures using new constitutive models. *Comput Struct.* 2001;79(32):2781-2791.
 11. Ngo D, Scordelis AC. Finite element analysis of reinforced concrete beams. *J ACI.* 1967;64:152-163.
 12. Blaauwendraad J. Realisations and restrictions—application of numerical models to concrete structures. In: Meyer C, Okamura H, eds. *Finite element analysis of reinforced concrete structures*. New York, NY: ASCE; 1985:557-578. Proceeding of US-Japan Seminar.
 13. Ingraffea AR, Saouma V. Numerical modelling of discrete crack propagation in reinforced and plain concrete. In: *Fracture Mechanics of Concrete*. Springer: the Netherlands. Vol 4; 1985:171-225.
 14. Koutromanos I, Shing PB. A cohesive crack model to simulate cyclic response of concrete and masonry structures. *ACI Struct J.* 2012;109:349-358.
 15. Schlangen E, Van Mier JGM. Experimental and numerical analysis of the micro-mechanisms of fracture of cement-based composites. *Cem Concr Compos.* 1992;14:105-118.
 16. Tuniki BK. Peridynamic Constitutive Model for Concrete [MS dissertation]. New Mexico: University of New Mexico; 2012.
 17. Van Mier JGM. *Concrete Fracture a Multiscale Approach*. Boca Raton, FL: CRC; 2013.
 18. Cusatis G, Bazant ZP, Cedolin L. Confinement-shear lattice model for concrete damage in tension and compression: I. Theory. *ASCE J Eng Mech.* 2003;129:1439-1448.
 19. Schlaich J, Schäfer K, Jennewein M. Toward a consistent design of structural concrete. *J Prestressed Concr Inst.* 1987;32(3):74-150.
 20. Hrennikoff A. Solution of problems of elasticity by the framework method. *J Appl Mech Tech Phys.* 1941;12:169-175.
 21. Silling SA. Reformulation of Elasticity Theory for Discontinuities and Long-Range Forces. Technical Report SAND98-2176, Sandia National Laboratories, Albuquerque, NM; 1998.
 22. Silling SA, Bobaru F. Peridynamic modeling of membranes and fibers. *Int J Nonlinear Mech.* 2005;40:395-409.
 23. Silling SA, Epton M, Weckner O, Xu J, Askari A. Peridynamics states and constitutive modeling. *J Elasticity.* 2007;88:151-184.
 24. Mitchell JA. A nonlocal, ordinary, state-based plasticity model for peridynamics. SAND2011-3166. Sandia National Laboratories, Albuquerque, NM; 2011.
 25. Gerstle W, Sau N, Silling SA. Peridynamic modeling of plain and reinforced concrete structures. 18th International Conference on Structural Mechanics in Reactor Technology (SMIRT 18), Beijing, China, SMIRT18-B01-2; 2005, 1–18.
 26. Kröner E. Elasticity theory of materials with long range cohesive forces. *Int J Solid Struct.* 1967;3:731-742.
 27. Eringen AC. Vistas of nonlocal continuum physics. *Int J Eng Sci.* 1992;30(10):1551-1565.
 28. Kunin IA. *Elastic Media with Microstructure*. Berlin: Springer; 1982.
 29. Macek WM, Silling SA. Peridynamics via finite element analysis. *Finite Element Anal Des.* 2007;43:1169-1178.
 30. Rots JG. Sequentially linear continuum model for concrete fracture. In: de Borst R, Mazars J, Pijaudier-Cabot G, van Mier JGM, Balkema AA, eds. *Fracture Mechanics of Concrete Structures*. Vol 2. Lisse, The Netherlands: CRC Press; 2001:831-839.
 31. Gopalaratnam VS, Shah SP. Softening response of plain concrete in direct tension. *ACI J.* 1985;3:310-323.
 32. Cornelissen HAW, Hordijk DA, Reinhardt HW. Experimental determination of crack softening characteristics of normal weight and lightweight concrete. *Heron.* 1986;31(2):45-56.
 33. Bhattacharjee SS, Leger P. Application of NLFM models to predict cracking in concrete gravity dams. *J Struct Eng.* 1994;120(4):1255-1271.
 34. Feenstra PH, de Borst R. A composite plasticity model for concrete. *Int J Solids Struct.* 1996;33(5):707-730.
 35. Park H, Klingner RE. Nonlinear analysis of RC members using plasticity with multiple failure criteria. *J Struct Eng.* 1997;123(5):643-651.
 36. Petersson PE. II Crack Growth and Development of Fracture Zones in Plain Concrete and Similar Materials. II Report TVBM-1006, Division of Building Materials, Lund Institute of Technology, Lund, Sweden; 1981.
 37. Aldemir A, Binici B, Arici Y, Kurc O, Canbay E. Pseudo-dynamic testing of a concrete gravity dam. *Earthq Eng Struct Dyn.* 2015;44:1747-1763.
 38. Gijsbers FB, Hehemann AA. Some Tensile Tests on Reinforced Concrete. Report BI-77-61, TNO Institute for Building Materials and Structures, Delft, The Netherlands; 1977.

39. Walraven, J.C.: The Influence of Depth on the Shear Strength of Light-weight Concrete Beams Without Shear Reinforcement. Report 5-78-4, Stevin Laboratory, Delft University of Technology, Delft; 1978.

AUTHOR'S BIOGRAPHIES



Beyazit B. Aydin, MSc
Department of Civil Engineering
Middle East Technical University
Ankara, Turkey
beyazit@metu.edu.tr



Professor Kagan Tuncay
Department of Civil Engineering
Middle East Technical
University Ankara, Turkey
tuncay@metu.edu.tr



Professor Baris Binici
Department of Civil Engineering
Middle East Technical University
Ankara, Turkey
binici@metu.edu.tr

How to cite this article: Aydin BB, Tuncay K, Binici B. Overlapping Lattice Modeling for concrete fracture simulations using sequentially linear analysis. *Structural Concrete*. 2017;1–14. <https://doi.org/10.1002/suco.201600196>